

Design and evaluation of a 433 MHz LoRa-based wireless communication system for agricultural monitoring

Jarosław Tatarczak¹ 

¹ Faculty of Mathematics and Information Technology, Lublin University of Technology, 20-618 Lublin, Poland
E-mail: j.tatarczak@pollub.pl

ABSTRACT

This article presents the design and experimental evaluation of a low-cost data transmission system based on LoRa technology (433 MHz) for applications in precision agriculture. The aim of the study was to design, implement, and test a low-cost, energy-efficient system capable of wirelessly transmitting information from sensors deployed in agricultural fields—such as soil moisture, temperature, and sunlight data. The tests were conducted with three transmission rates (0.1, 1.0, and 10 kbps) and varying bandwidths and spreading factors. The results showed that transmission at 0.1 kbps with bandwidths of 7.8 kHz and 20.8 kHz achieved less than 1% packet loss up to 150 m. However, this configuration required up to 140 times higher energy consumption compared with high-rate settings (10 kbps). At 10 kbps, almost all packets failed to reach the receiver at distances exceeding 100 m. Variations in reception between test paths were observed and were attributed to terrain and structural conditions (e.g., building reflections), which affected both RSSI and SNR values. The results demonstrate that LoRa technology operating at 433 MHz can provide a reliable foundation for autonomous, distributed monitoring systems in agriculture. This study provides novel quantitative evidence of how specific transmission parameters influence the trade-off between communication reliability and energy efficiency under real field conditions. The findings offer practical guidelines for designing optimized LoRa-based telemetry systems, supporting more informed decision-making in irrigation, fertilization, and crop protection.

Keywords: wireless transmission, low-cost system, LoRa, precision agriculture.

INTRODUCTION

The growth of the global population and the increasing demand for food necessitate the implementation of advanced technologies in agriculture. Traditional cultivation methods often prove insufficient in addressing the challenges of production optimization, natural resource conservation, and loss minimization. In response to these demands, precision agriculture has emerged, integrating advanced measurement, analytical, and communication tools to enhance the efficiency of resource management.

This manuscript is structured as follows: first, it introduces the background and wireless communication methods relevant to precision agriculture, with particular emphasis on LoRa technology. Next, it presents the experimental setup

and methodology, followed by the results and discussion. The paper concludes with a summary of findings and future research directions.

An essential component of precision agriculture is crop telemetry, which enables the remote, real-time monitoring of environmental parameters and plant conditions [1]. The implementation of telemetry solutions in agriculture allows for the automation of data collection processes, eliminating the need for manual measurements and enhancing the accuracy of analyses. Automating data acquisition is particularly important for large-scale farms, where traditional monitoring methods can be time-consuming and inefficient [2]. To an increasing extent, this is achieved through the use of a technology known as the internet of things (IoT), which enables the integration of numerous sensors and devices into a

single intelligent network capable of collecting and transmitting data in real time [1, 3]. Continuous access to current data empowers farmers to make more informed decisions regarding irrigation, fertilization, and crop protection, ultimately leading to increased yields and reduced costs and resource consumption [3].

As part of telemetry measurements, a variety of key parameters can be monitored [1], such as soil moisture, air temperature, sunlight intensity, carbon dioxide concentration, nutrient content in the soil, and precipitation levels. This data enables the precise adjustment of cultivation conditions to meet the specific needs of targeted crops, thereby minimizing losses and increasing production efficiency. Various wireless communication technologies can be used to transmit telemetry data. In addition to LoRa, technologies such as Wi-Fi, Bluetooth, Zigbee, cellular networks (LTE, 5G), and satellite communication are also employed [4]. Each of these technologies has its own advantages and limitations—for example, Wi-Fi and Bluetooth are suitable for small areas with high device density; LTE and 5G offer high bandwidth but require access to operator infrastructure; while satellite systems allow communication in the most remote locations, although they are associated with high costs (Table 1).

The LoRa (long range) technology [6] is particularly advantageous for precision agriculture [9], as it enables long-distance data transmission (ranging from several to over a dozen kilometers) while maintaining very low power consumption. This is crucial in distributed measurement systems, where powering sensing devices directly

from the electrical grid may be limited. Moreover, LoRa-based radio transmission operates within unlicensed ISM (Industrial, Scientific, Medical) frequency bands [10], potentially eliminating additional costs related to transmission fees, as is often the case with cellular networks. Another benefit is the independence from cellular network access, which can be especially significant in sparsely populated areas.

Despite its numerous advantages, LoRa technology also has some limitations. Most notably, its relatively low data rate (measured in kbps) [6], making it unsuitable for transmitting large volumes of data, such as audio, images, or video. Due to this low data rate, the technology is insufficient for real-time communication system. An additional challenge is the potential for interference from other devices operating within the similar frequency band. In scenarios with intensive use of the technology, this can lead to a decline in radio transmission quality.

The selection of the communication technology in this study was guided by several key criteria: autonomous and maintenance-free operation, low power consumption, long transmission range, and the absence of a requirement for real-time data transfer, which makes low data rates non-problematic. An equally important factor was the use of license-free ISM frequency bands, ensuring independence from external data transmission infrastructures. These requirements are well met by LoRa technology, which combines energy efficiency with long-range communication in unlicensed frequency bands, making it particularly suitable for agricultural telemetry applications.

Table 1. Comparison of different wireless radio transmission technologies

Radio transmission technology	Frequency	Range (outside)	Bit rate	Electricity demand	Cost	Source
LoRaWAN	433 MHz 868 MHz 915 MHz	< 30 km	< 50 kbps	Low	Low	[5, 4, 6]
ZigBee	868 MHz 915 MHz 2.4 GHz	< 100 m	< 250 kbps	Low	Low	[4]
WiFi	2.4 GHz 5 GHz	< 100 m	< 150 Mbps	High	Medium	[4]
SigFox	433 MHz 862 MHz 928 MHz	< 40 km	< 100 bps	Low	Low	[5]
Bluetooth	2.4 GHz	<10 m	< 3 Mbps	Low	Medium	[7, 4]
Cellular networks (2G/3G/4G/5G)	0.8 – 3.6 GHz	< 10 km	< 10 Mbps	Medium	Low	[4]
Ultra-Wideband (UWB)	3.1–4.8 GHz 6–8.5 GHz	< 100 m	> 100 Mbps	Low	Medium	[8]

The Table 2 presents a list of scientific publications referring to the above criteria related to LoRa technology in agricultural applications:

The aim of this article is to analyze the quality of telemetry data transmission for the needs of precision agriculture using LoRa modules. The study is based on measurements conducted under real-world conditions. It discusses both the fundamental principles of this technology and the factors that affect communication stability and reliability in agricultural environments. Various combinations of remote transmission parameters were tested using LoRa modules in field conditions. Furthermore, the amount of electrical energy required to transmit a single unit of data (byte) was estimated.

The novelty of this study lies in the experimental evaluation of low-cost LoRa-based telemetry in a rural agricultural environment at 433 MHz, with a focus on analyzing the relationship between transmission settings (for 0.1, 1.0, 10 kbps data rate), communication reliability (RSSI, SNR, packet delivery), and energy consumption (per 50 bytes of data). The results provide empirical evidence on how environmental conditions and transmission parameters interact, offering practical insights into the deployment of energy-efficient telemetry systems for precision agriculture.

What is LoRa technology?

LoRa technology derives its name from the words “Long” and “Range,” which reflect its long-range communication capabilities. The technology itself uses chirp spread spectrum (CSS) modulation, which serves as the physical layer for data transmission [18, 19]. In this modulation technique, frequency-modulated pulses, known as “chirps”, are used to transmit information. The graphic below (Figure 1) shows the spectrogram

of radio signal at the physical layer using CSS modulation in LoRa technology.

Each radio transmission in LoRa technology begins with the transmission of a preamble, which serves to synchronize the receiving station with the incoming radio signal [20, 19]. The length of the preamble can vary, and extending it may be beneficial when transmitting over long distances. The next element of the transmission is the synchronization word (identification address), which allows the receiver to recognize the type of network. The synchronization word can be up to 8 bytes in length (typically 2 or 4 bytes) [19].

Following the synchronization word, a header may be included, containing basic information about the transmitted data (payload), such as the number of bytes and whether CRC checking is enabled [19]. After the header comes the payload section, which carries the actual information. The theoretical maximum size of the payload is 255 bytes; however, when a header or additional coding schemes (e.g., Spread Factor = 12) are used, the actual maximum size may be smaller.

Range vs radio frequency

The range of radio transmission can be described using the Friis transmission equation [21], which models wave propagation in free space (ideal conditions). In free space, signal power decreases according to the inverse square law of distance.

$$P_r = P_t \cdot G_t \cdot G_r \left(\frac{\lambda}{4\pi d} \right)^2 \quad (1)$$

where: P_r – received signal strength (W), P_t – transmitter power (W), G_r – receiving antenna gain, G_t – transmitting antenna gain, λ – wavelength (m), d – free path between antennas (m).

Table 2. Scientific publications related to the use of LoRa technology in agriculture

Author	Ref. no.	Research area in agriculture	LoRa frequency
Ojo et al.	[11]	Wildlife monitoring in a forest vegetation area	433 MHz 868 MHz
Liang et al.	[12]	Signal propagation on tea plantation	433 MHz
Xu et al.	[13]	Signal propagation on maize plantation	433 MHz
Guzmán et al.	[14]	Signal propagation on crops located in mountainous areas	915 MHz
Enock et al.	[15]	Real-time monitoring, controls irrigation and signal propagation	433 MHz
Tan et al.	[16]	Signal propagation on the eucalyptus plantation	433 MHz
Anzum et al.	[17]	Signal propagation on oil palm plantation	433 MHz

After transforming the equation and inserting

$$d = \frac{c}{4\pi f} \sqrt{\frac{P_t \cdot G_t \cdot G_r}{P_r}} \quad (2)$$

The distance between two antennas is inversely proportional to the operating frequency of the radio device under free-space conditions. This is a key factor when selecting the appropriate operating frequency for a data transmission system intended for agricultural use. The average agricultural land area per farm owner in Poland is 11.59 hectares (0.1159 km²) [22]. Assuming ideal conditions in which the entire cultivated area forms a uniform circular region with the farm located at its center, the maximum distance from the center to the edge of this area is approximately 192 meters, based on the mean value in Poland. In reality, the distance a farmer must travel to reach their fields can be significantly greater. In this study, a maximum measurement distance of 200 meters between the transmitter and receiver was used as the starting point for field tests. Obstacles in agricultural environments, such as vegetation, buildings, or terrain, can significantly affect the quality of radio transmission [23]. Lower frequencies (e.g., LoRa 433 MHz or 868 MHz) are better at penetrating obstacles, while higher frequencies (e.g., Wi-Fi 5 GHz) offer higher bandwidth but are more susceptible to signal attenuation.

Legal regulations

According to Polish legal regulations set out in the Prawo komunikacji elektronicznej of July 12, 2024 [24], all radio devices intended solely for receiving radio signals are exempt from licensing

requirements (Article 145, paragraph 1). However, radio devices using LoRa protocols are designed for both transmitting and receiving radio signals. The legislator has created a facility to enable the legal use of such devices. This is addressed in Article 145, paragraph 5, which states that transceiver devices classified as Class 1 are exempt from licensing requirements. Class 1 radio devices are defined in Article 274, paragraph 3 as: “radio equipment for which Member States do not apply restrictions regarding placing on the market or putting into service.” On the Public Information Bulletin (pl. Biuletyn Informacji Publicznej – BIP) website of the Office of Electronic Communications (pl. Urząd Komunikacji Elektronicznej – UKE), an example list of Class 1 devices can be found [25]. This list includes the subclass, device type, and frequency range. Additionally, the BIP UKE website references Commission Decision 2000/299/EC (Article 1(3)), which includes a table listing equipment covered under the scope of Class 1 devices [26]. The list contains 126 examples of Class 1 radio communication devices. Each entry provides details such as application, frequency band, transmission power or power density, and other information regarding typical use cases for such radio equipment.

The 169 MHz radio band is rarely used for communication via LoRa protocols. The 433 MHz band, however, is mainly used for transmitting telemetry data. It is not recommended to transmit audio or video data over this band. The 868 MHz band can be used to carry audio or video data.

The wireless transmission quality tests described in this paper were conducted in the

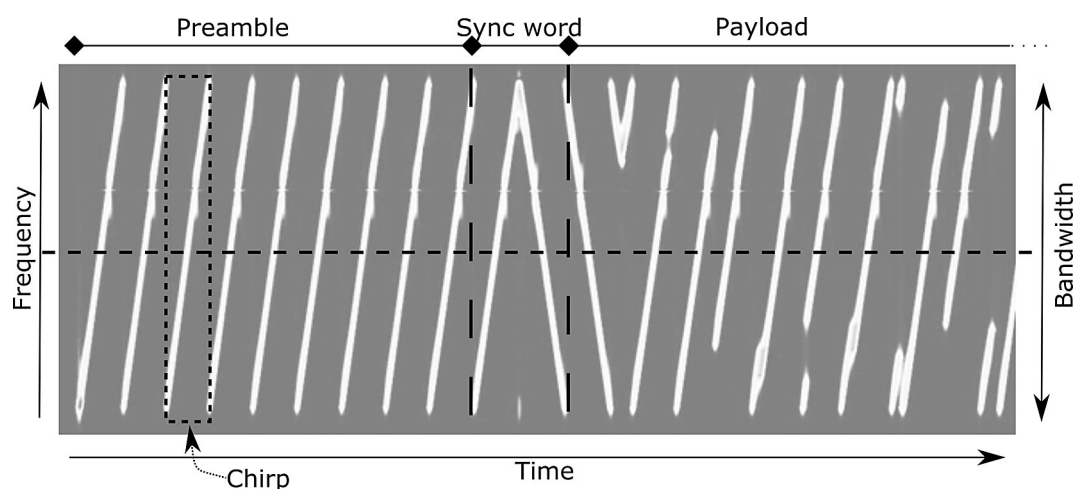


Figure 1. Spectrogram of the radio signal transmitted using CSS modulation. Transmission parameters: BW = 7.8 kHz, SF = 12

frequency range of 434.04–434.79 MHz (subclass 65), specifically using a frequency of 434.415 MHz (the center of the subclass 65 range). According to national regulations, the maximum permissible transmission power of a radio system operating in this band must not exceed 10 mW e.r.p. (for subclass 65), which corresponds to 10 dBm on a logarithmic scale.

Radiated radio power

The radiated power of a radio system consists of the transmitter power, antenna gain, and losses in the cables/connectors between the antenna and the transmitter. In the experiment, the Ra-02 radio module was used [27]. A 10 cm IPX-to-SMA adapter was placed between the antenna and the radio module. A 5 dBi monopole antenna with an SMA connector was used (Table 3). The effective radiated radio power (ERP), using dipole antennas, can be calculated using the following equation:

$$ERP = P_{TX} + G_A - L_C \quad (3)$$

where: P_{TX} – transmitter power (mW), G_A – antenna gain (dBi), L_C – signal losses on connectors and cables (dB).

By rearranging the above equation, it is possible to determine the maximum transmit power of the radio transmitter (P_{TX}) that allows transmission in compliance with the applicable regulations in Poland (with connector losses estimated at $L_C = 0.3$ dB):

$$P_{TX} = ERP - G_A + L_C \quad (4)$$

$$P_{TX} = 10 \text{ dBm} - 5 \text{ dBi} + 0.3 \text{ dB} \quad (5)$$

$$P_{TX} = 5.3 \text{ dBm} \approx 3.4 \text{ mW} \quad (6)$$

Table 3. Basic technical parameters of the Ra-02 radio module [27]

Model	Ra-02
Producent	Ai-Thinker
Interface	SPI
Frequency range	410-525 MHz
Antena socket	IPEX
Max transmit power	18+/- 1 dBm
Power (typical values) 433 MHz	TX: 93 mA, RX: 12.15 mA, Standby: 1.6 mA
Supply voltage	typ. 3.3 V
Modulation modes	FSK, GFSK, MSK, GMSK, LoRa™, OOK

In summary, the maximum transmit power of the radio transmitter (P_{TX}) should not exceed 5.3 dBm. For the purposes of further analysis, the transmit power of the radio module was set to 5.0 dBm. This is due to the technical limitations of the Ra-02 modules, where the transmission power is programmable in 1.0 dBm increments.

Bit rate calculation

The bit rate (BR) of radio transmission (in bps) using LoRa modules can be expressed by the following formula [19]:

$$BR = \frac{SF \cdot \frac{4}{4+CR} \cdot BW}{2^{SF}} \quad (7)$$

where: SF – spreading factor (7, 8, 9, 10, 11, 12), CR – coding rate (1, 2, 3, 4); BW – bandwidth (7.8, 10.4, 15.6, 20.8, 31.25, 41.7, 62.5, 125, 250, 500; unit: kHz).

Calculations of the transmission bit rate for a coding rate of $CR = 1$ (4/5) were used to prepare Table 4. Based on this table, it can be observed that the highest transmission speed is achieved with parameters $SF = 7$ and $BW = 500$ kHz, while the lowest speed corresponds to $SF = 12$ and $BW = 7.8$ kHz. It was assumed that the following data transmission rates would be examined in this study: 0.1, 1.0, and 10.0 kbps. Parameter combinations for the Ra-02 module settings (S1-S6) were selected to closely match the values from Table 4. The combinations of radio module settings are presented in the Table 5.

Transmission time analysis

In this part of the experiment, the total radio transmission time of a data frame with a payload length of 50 bytes was measured at a coding rate (CR) of 1 (4/5). The data frame preamble consisted of 8 symbols (software default setting). No checksum (CRC) or header information was transmitted in the data frame. The time was measured using a NodeMCU (ESP8266) controller. The results are presented in Table 6.

Electricity consumption

Electric power consumption of the radio module depends on the following factors: operating mode (transmission, reception, or standby), programmable power level of the radio module, and device operating time. In the study, an experiment

Table 4. The LoRa radio transmission bit rate, determined for a coding rate of CR = 1, is expressed in kbps

Parameter		Spread Factor (SF)					
		7	8	9	10	11	12
Bandwidth (BW), kHz	7.8	0.34	0.2	(S1) 0.11	0.06	0.03	0.02
	10.4	0.46	0.26	0.15	0.08	0.04	0.02
	15.6	0.68	0.39	0.22	0.12	0.07	0.04
	20.8	0.91	0.52	0.29	0.16	(S2) 0.09	0.05
	31.25	1.37	0.78	0.44	0.24	0.13	0.07
	41.7	1.82	(S3) 1.04	0.59	0.33	0.18	0.1
	62.5	2.73	1.56	0.88	0.49	0.27	0.15
	125	5.47	3.13	1.76	(S4) 0.98	0.54	0.29
	250	(S5) 10.94	6.25	3.52	1.95	1.07	0.59
	500	21.88	(S6) 12.5	7.03	3.91	2.15	1.17

Table 5. List of chosen radio transmission settings parameters selected for the study

Setting	S1	S2	S3	S4	S5	S6
Bandwidth (BW), kHz	7.8	20.8	41.7	125	250	500
Spread Factor (SF)	9	11	8	10	7	8
Bit Rate, kbps	0.11	0.09	1.04	0.98	10.94	12.5
	~ 0.1 kbps		~1.0 kbps		~10.0 kbps	

was conducted measuring the electric current of the transmitter during radio transmission at a programmable power of 5 dBm. The measurement was performed using an Agilent 34461A device. The results showed an increase in the transmitter's current consumption by 30.1 mA. With a supply voltage of 5.0 V DC, this corresponds to an electric power consumption of 150.5 mW. This is the power consumed by the Ra-02 transmitter module during radio transmission using a 5 dBi monopole antenna. Below is the electric energy

consumption for a single transmission of 50 bytes (+ preamble) of data with different combinations of Ra-02 module transmission settings (Table 7).

MATERIALS AND METHODS

The study was conducted in a rural area located in the Lublin Voivodeship. The village features typical rural development with elements of

Table 6. Measured radio transmission duration (preamble + 50 bytes payload) depending on BW and SF parameters, values expressed in milliseconds

Parameter		Spread Factor (SF)					
		7	8	9	10	11	12
Bandwidth (BW), kHz	7.8	1 644	3 614	(S1) 6 571	11 830	21 038	39 454
	10.4	1 233	2 711	4 929	8 873	15 779	29 590
	15.6	822	1 480	3 286	5 916	10 520	19 728
	20.8	617	1 111	2 465	4 437	(S2) 7 891	14 796
	31.25	412	741	1 316	2 959	5 260	9 865
	41.7	309	(S3) 556	987	2 219	3 945	7 398
	62.5	207	371	659	1 234	2 631	4 933
	125	104	186	330	(S4) 618	1 153	2 467
	250	(S5) 53	94	166	310	576	1 070
	500	26	(S6) 47	83	156	289	536

suburban infrastructure. The maximum distance between the transmitting and receiving stations was 200 meters. The study employed two radio devices (a transmitter and a receiver), built from modular components and programmed with dedicated code (C++). The GPS module was controlled via a UART bus, the OLED display via an I2C bus, and the LoRa module and SD card module via an SPI bus. The entire system was assembled on a breadboard and powered by a wireless power source. The LoRa module settings were configured using an infrared remote control. The Table 8 presents a list of components used in the construction of the radio devices: The following parameters were measured in the study:

- received signal strength indicator – RSSI (dBm),
- signal-to-noise ratio – SNR (dB),
- number of correctly received data packets (frames) – a packet is considered correct if its contents exactly match the transmitted value; packets not received at all or only partially are excluded.

The distance between the transmitting and receiving stations was determined using the formula

describing the distance between two points on a sphere (the Haversine formula) [28]:

$$d = 2r \cdot \arcsin \left(\sqrt{\sin^2 \left(\frac{\Delta\varphi}{2} \right) + \cos\varphi_1 \cdot \cos\varphi_2 \cdot \sin^2 \left(\frac{\Delta\lambda}{2} \right)} \right) \quad (8)$$

where: r – mean radius of the Earth (6371 km),
 $\Delta\varphi$ – difference in latitude between points,
 $\Delta\lambda$ – difference in longitude between the points, φ_1 – latitude of the first point, φ_2 – latitude of the second point.

The study assumed a unidirectional data flow between transmitter and receiver. The picture below (Figure 2) presents an overview map of the experimental area. The study was conducted as follows:

1. The base point (receiving station) was set in the central part of the experimental area (point A), mounted on a tripod at a height of 1.2 meters above ground level.
2. At point B, a person walked slowly toward point A, holding the transmitting station in their hands at a height of 1.2 meters above ground level.
3. The movement was directed from point B to

Table 7. Electric power consumption for selected radio transmissions settings

Setting	BW	SF	BR	Transmission time	Electric energy for transmitting 50 bytes		Energy consumption assuming transmission every 15 minutes (96 times/day)		
	kHz	-	kbps	s	mWh	J	mWh/day	mWh/week	mWh/month
S1	7.8	9	0.11	6.571	0.275	0.989	26.372	184.601	791.148
S2	20.8	11	0.09	7.891	0.330	1.188	31.669	221.684	950.076
S3	41.7	8	1.04	0.556	0.023	0.084	2.231	15.620	66.942
S4	125	10	0.98	0.618	0.026	0.093	2.480	17.362	74.407
S5	250	7	10.94	0.053	0.002	0.008	0.213	1.489	6.381
S6	500	8	12.5	0.047	0.002	0.007	0.189	1.320	5.659

Table 8. List of components used in the study along with their purchase cost

Transmitter		Receiver	
Component type	Cost PLN	Component type	Cost PLN
Controller – NodeMCU (ESP8266)	25	Controller – NodeMCU (ESP8266)	25
Radio module – Ra-02 (LoRa) + adapter IPEX-SMA + antenna 5 dBi	55	Radio module – Ra-02 (LoRa) + adapter IPEX-SMA + antenna 5 dBi	55
Real time module – ZS-042 (DS3231)	20	SD module + SD card	35
Geolocation module - GY-GPS6MV2 (NEO6MV2)	30	Geolocation module - GY-GPS6MV2 (NEO6MV2)	30
OLED 0,96" display (64x128px)	20	OLED 0,96" display (64x128px)	20
Solderless breadboard	10	Solderless breadboard	10
Infrared receiver + remote control	15		
=	160	=	175

point A. The distance between points B and A was 200 meters. The interval (time without radio transmission) between consecutive radio transmissions was 1 second.

4. After completing one measurement series, the transmission parameters were changed (according to Table 5), and the entire procedure was repeated.
5. After completing the study for all combinations of the radio module settings, the measurement location was changed from points B-A to D-C, and the entire procedure was repeated.

The elevation data above sea level was obtained from the digital terrain model (DTM1) database with a 1×1 m grid resolution [29]. The height difference between points B and A was 2.9 meters, while the difference between points D and C was 2.8 meters. This means that the average terrain slope over the B–A segment was 1.45%, and over the D–C segment it was 1.4%. The measurements were conducted on a day with low cloud cover, a temperature of approximately 15 °C, 50% relative humidity, wind velocity below 4 m/s, and a planetary K-index ≤ 2.0 .

RESULTS

Based on the conducted study, RSSI and SNR characteristics as a function of distance were generated, as shown in the Figures 3–6.

Based on Figure 3 and Figure 4, it can be observed that the RSSI values change exponentially with the distance between the transmitting and receiving stations. In Figure 5 and Figure 6, it is evident that the SNR values for configurations S1 and S2 exhibit an almost linear trend along the B–A segment. For configuration S1, the SNR does not drop below 10 dB, which indicates a high signal level relative to ambient noise. The lowest SNR level can be observed for configuration S6. This is due to the use of a 500 kHz bandwidth in this configuration, which is more susceptible to interference compared to the bandwidths used in the other configurations. The charts below (Figure 7) present the measured RSSI and SNR values categorized into four distance classes from the receiving station: up to 50 m, 50–100 m, 100–150 m, and 150–200 meters. Based on Figure 7, a significant decrease in signal strength with increasing distance between the transmitting and receiving stations can be observed. For the B–A segment, the RSSI is generally higher compared to the D–C segment. In the case of configurations S5 and S6, within the 100–150 m and 150–200 m ranges for the D–C direction, data gaps can be observed, caused by either incomplete or completely missing data frame deliveries. Based on Table 9, it can be observed that a distance of up to 50 meters between the transmitting and receiving stations guarantees correct data transmission regardless of the combination of radio transmission parameter settings. The setting combinations S1

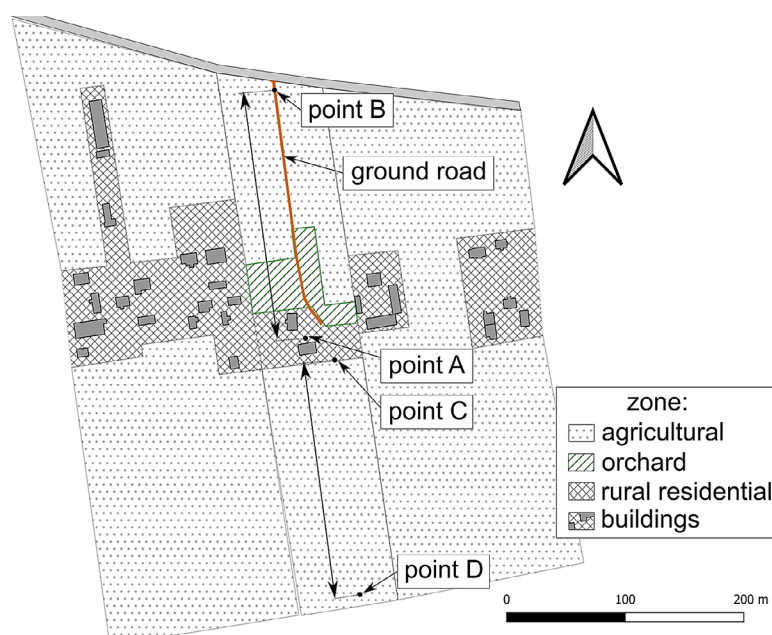


Figure 2. Experimental area with indicated locations of the transmitter and receiver stations

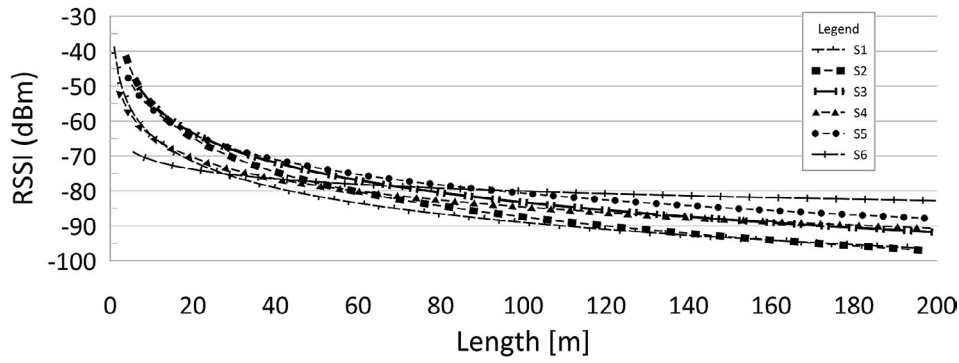


Figure 3. Dependence of the RSSI on distance along the B–A segment

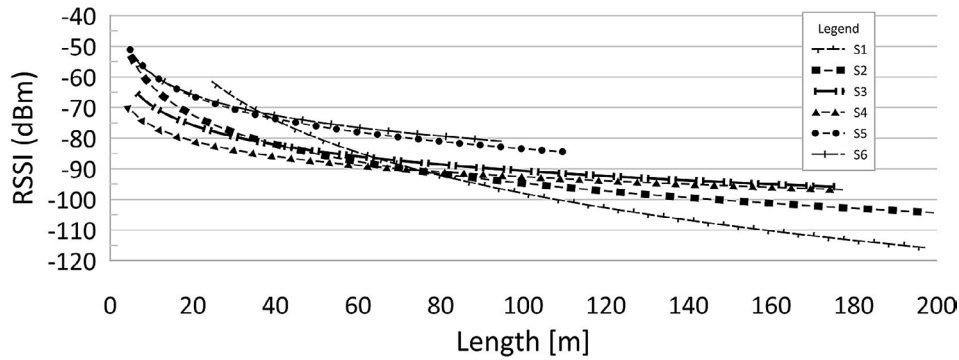


Figure 4. Dependence of the RSSI on distance along the D–C segment

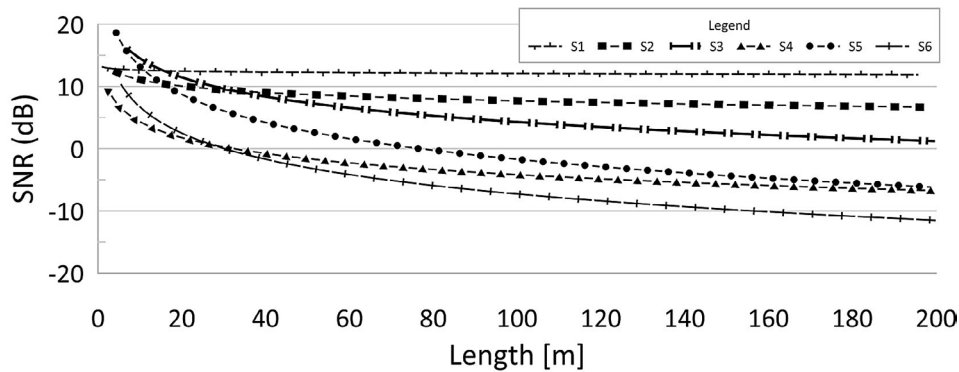


Figure 5. Dependence of the SNR on distance along the B–A segment

and S2 highly ensure correct data transmission at distances up to 200 meters.

In the case of the measurement on segment D-C, it can be observed that the percentage of correctly delivered data frames is lower than on segment B-A. This difference may result from the location of the receiving station (Figure 2). For segment B-A, there was a building wall behind the receiving station, with a distance of 3 meters between the building and the receiving station. The building wall could have reflected part of the radio waves, thereby increasing the signal strength reaching the radio receiver.

Discussion

The analysis of the measurements in this study demonstrated clear relationships between transmission parameters, distance, and communication reliability. Specifically, lower data rates (0.1 kbps) combined with bandwidths of 7.8 kHz and 20.8 kHz resulted in minimal packet loss over distances up to 150 meters, whereas higher data rates (10 kbps) caused almost complete packet loss beyond 100 meters. This highlights the trade-off between energy efficiency and data reliability in low-power wireless systems. While no directly comparable

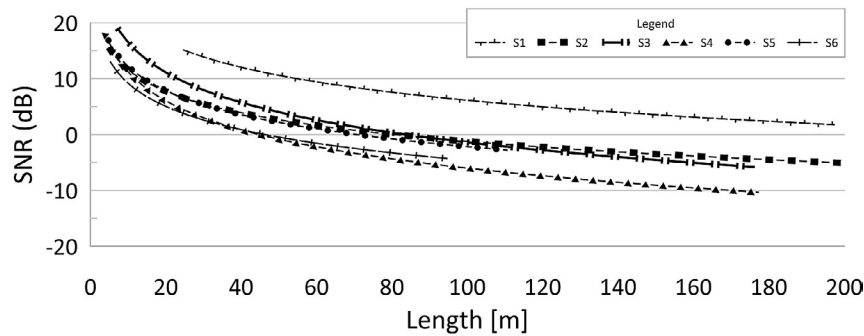


Figure 6. Dependence of the SNR on distance along the D-C segment

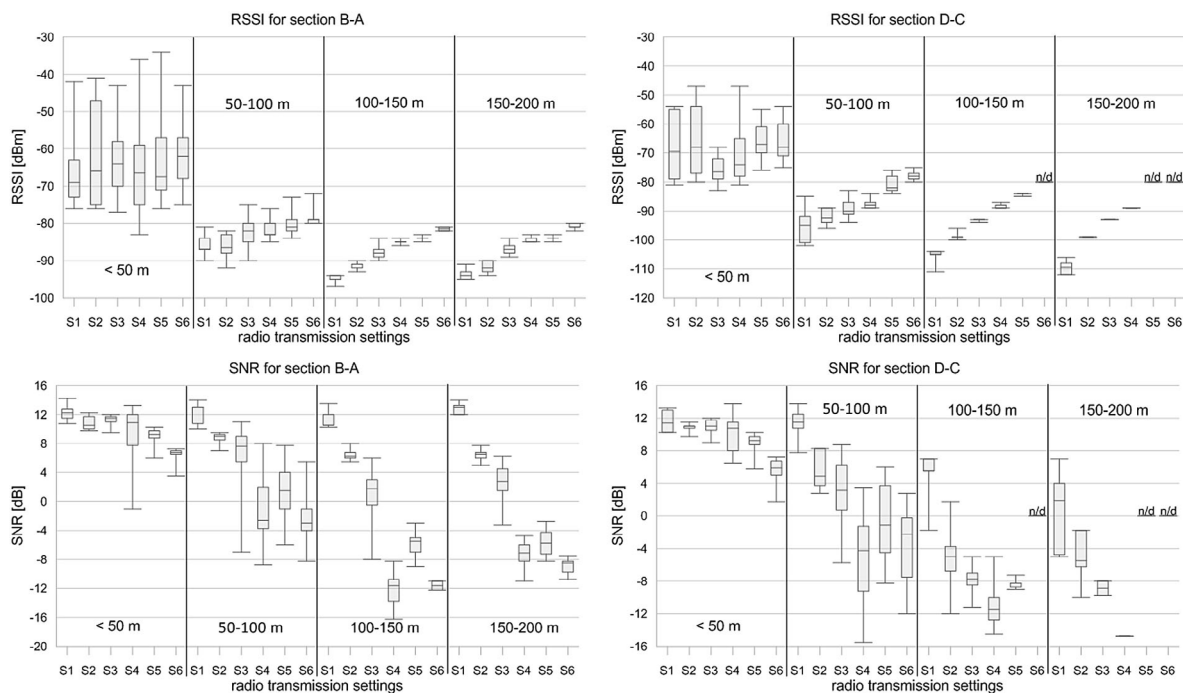


Figure 7. RSSI and SNR values categorized by distance classes for the two measurement segments: B-A and D-C

research has been identified, several recent studies have examined related concepts in adjacent domains. In the study by Ojo et al. [11], a solution was presented in which radio signal propagation was investigated in a forested area. In contrast, Xu et al. [13] conducted measurements using only a single combination of radio module configuration and higher transmitter power (20 dBm). Guzmán et al. [14] described measurements in mountainous terrain and at the 915 MHz band, differing from the present study, which was conducted in nearly flat (slope < 1.45%) terrain at 433 MHz frequency band. Enock et al. [15] presented a system for data collection and irrigation control, involving two-way communication and a transmitter power of 20 dBm—approximately 32 times higher than in the current study. Tan et al. [16] and Anzum et

al. [17] described signal propagation in eucalyptus and oil palm plantations, respectively, considering terrain obstacles. In the present work, however, crop fields (cereals) were in an early growth stage and did not constitute obstacles between the transmitting and receiving stations. Additionally, this study analyzed six different combinations of module settings matched to data rates of 0.1, 1.0, and 10 kbps.

These observations demonstrate that careful selection of transmission parameters is crucial to maintain reliable communication while minimizing energy consumption. Moreover, the findings indicate that local environmental conditions must be considered when deploying LoRa-based telemetry systems in agricultural fields. The demonstrated framework can be adapted to other application

Table 9. Percentage of correctly delivered data frames by distance class between transmitter and receiver on the B–A and D–C segment

Setting	distance (m) at segment B-A				distance (m) at segment D-C			
	< 50	50-100	100-150	150-200	< 50	50-100	100-150	150-200
S1	100%	100%	100%	100%	100%	100%	100%	88%
S2	100%	100%	100%	100%	100%	100%	100%	80%
S3	100%	100%	100%	100%	100%	100%	45%	10%
S4	100%	95%	68%	100%	100%	92%	48%	4%
S5	100%	90%	71%	90%	100%	97%	20%	0%
S6	100%	94%	7%	60%	100%	80%	0%	0%

domains, including environmental monitoring, smart infrastructure, and industrial IoT, where similar trade-offs between energy consumption, coverage, and data reliability are critical.

CONCLUSIONS

Based on the results presented above, this study provides practical guidance for designing energy-efficient and reliable LoRa-based telemetry systems, thereby contributing to the advancement of precision agriculture and low-power wireless communication research. The following conclusions can be drawn:

- The radio transmission bit rate and the distance between the transmitting and receiving stations significantly affected the quality of the radio communication.
- Transmission without or with minimal data packet loss was only possible with bandwidths of 7.8 kHz and 20.8 kHz, corresponding to configurations S1 and S2. These configurations assumed a transmission rate of 0.1 kbps. The disadvantage of this type of transmission was the significantly increased energy consumption required to send the data (up to 140 times more when comparing S1 to S6).
- As the radio transmission bit rate increased, the number of lost data packets also increased. In the case of series S6 on segment D-C, none of the data packets were received correctly at distances greater than 100 meters.
- Differences in the number of received data packets on segments B-A and D-C can be attributed to the presence of a building behind point B on segment B-A, which reflected some of the radio waves and may have enhanced the signal reaching the receiver.

- A system operating at a frequency of 433 MHz may find applications in agriculture; however, it requires further work on refining the appropriate radio transmission parameters.
- For future work, it is recommended to systematically investigate the impact of antenna height and type (omnidirectional vs. directional) on communication reliability. Field tests should include varying crop heights, orchards, and typical farm structures to quantify their effect on RSSI, SNR, and packet loss. Additionally, experiments optimizing LoRa transmission parameters (bit rate, bandwidth, spreading factor) under these conditions could guide the design of more robust and energy-efficient agricultural telemetry systems.

Acknowledgments

The grant was financed in the framework of the pro-quality program “Grants for Grants” (Grant no. 4/GnG2/2022) at the Lublin University of Technology.

REFERENCES

1. Dhanaraju M., Chenniappan P., Ramalingam K., Pazhanivelan S., Kaliaperumal R. Smart farming: internet of things (IoT)-based sustainable agriculture. *Agriculture*. 2022; 12(10), 1745. <https://doi.org/10.3390/agriculture12101745>
2. Kumar V., Sharma K.V., Kedam N., Patel A., Kate T.R., Rathnayake U. A comprehensive review on smart and sustainable agriculture using IoT technologies. *Smart Agric. Technol.* 2024; 8: 100487. <https://doi.org/10.1016/j.atech.2024.100487>
3. Duguma A.L. and Bai X. How the internet of things technology improves agricultural efficiency. *Artif. Intell. Rev.* 2025; 58: 63. <https://doi.org/10.1007/>

- s10462-024-11046-0
4. Soussi A., Zero E., Sacile R., Trihero D, Fossa M. Smart sensors and smart data for precision agriculture: A review. *Sensors*. 2024; 24(8): 2647. <https://doi.org/10.3390/s24082647>
5. Kuntke F., Sinn M., Reuter C. Reliable Data Transmission using Low Power Wide Area Networks (LPWAN) for Agricultural Applications. *ARES 2021: Proc. 16th Int. Conf. Availab. Reliab. Secur.* 2021; 35. <https://doi.org/10.1145/3465481.3469191>
6. Kamal M. A., Alam M. M., Sajak A. A. B., Mohd Su'ud M. Requirements, deployments, and challenges of LoRa technology: A survey. *Comput. Intell. Neurosci.* 2023; <https://doi.org/10.1155/2023/5183062>
7. Taşkın D., Taşkın C., Yazar S. Developing a Bluetooth low energy sensor node for greenhouse in precision agriculture as internet of things application. *Advances in Science and Technology Research Journal*. 2018; 12(4): 88–96. <https://doi.org/10.12913/22998624/100342>
8. Cicchetti R., Miozzi, E., Testa, O. Wideband and UWB antennas for wireless applications: A comprehensive review. *Inter. J. of Antennas and Propagation*. 2017; 15: 1–45. <https://onlinelibrary.wiley.com/doi/10.1155/2017/2390808>
9. Aldhaheeri L., Alshehhi N., Manzil I., Khalil R., Javaid S., Saeed N. LoRa Communication for agriculture 4.0: Opportunities, challenges, and future directions. *IEEE Internet Things J.* 2025; 12(2): 1380–1407. <https://doi.org/10.1109/JIOT.2024.3486369>
10. Kumbhar A. Overview of ISM Bands and Software-Defined Radio Experimentation. *Wirel. Pers. Commun.* 2017; 97: 3743–3756. <https://doi.org/10.1007/s11277-017-4696-z>
11. Ojo O. M., Adami D., Giordano S. Experimental evaluation of a lora wildlife monitoring network in a forest vegetation area. *Future Internet*. 2021; 13(5): 115. <https://doi.org/10.3390/fi13050115>
12. Liang Q., Tang P., Li H., Zhang Z., Pang Y., Zhang Y. Propagation characteristics of LoRa signal at 433 MHz channel in tea plantations. *Appl. Eng. Agric.* 2024; 40(3). <https://doi.org/10.13031/aea.15773>
13. Xu T., Ma D., Fang W., Huang Y. Experimental study on the propagation characteristics of LoRa signals in maize fields. *Electronics*. 2025; 14(11): 2156. <https://doi.org/10.3390/electronics14112156>
14. Rivera Guzmán, E. F., Mañay Chochos, E. D., Chiliquinga Malliquinga, M. D., Baldeón Egas, P. F., Toasa Guachi, R. M. LoRa network-based system for monitoring the agricultural sector in andean areas: Case study Ecuador. *Sensors*. 2022; 22(18): 6743. <https://doi.org/10.3390/s22186743>
15. Enock K.S., Sagali M.J., Jeannick U.I., Chen, D. LoRa-based smart agriculture monitoring and automatic irrigation system. *Journal of Computer and Communications*. 2025; 13: 1–20. <https://doi.org/10.4236/jcc.2025.133001>
16. Tan X., Yu X.-W., Zhang X., Li F., Liu Y., Ouyang X., Wen, Y. Propagation characteristics of LoRa signal at 433 mhz channel in eucalyptus plantation environment. *Journal of Forestry Engineering*. 2020; 5(2): 137–143. [10.13360/j.issn.2096-1359.201905012](https://doi.org/10.13360/j.issn.2096-1359.201905012)
17. Anzum R., Habaebi M. H., Islam M. R., Hakim G. P. N., Khandaker M. U., Osman H., Alamri S., Abdelrahim E. A Multiwall Path-Loss Prediction Model Using 433 MHz LoRa-WAN Frequency to Characterize Foliage's Influence in a Malaysian Palm Oil Plantation Environment. *Sensors*. 2022; 22(14): 5397. <https://doi.org/10.3390/s22145397>
18. Reynders B. and Pollin S. Chirp spread spectrum as a modulation technique for long range communication. *Symp. Commun. Veh. Technol. (SCVT)*, Mons, Belgium; 2016. <https://doi.org/10.1109/SCVT.2016.7797659>
19. Semtech. SX1276-7-8-9 Datasheet. April 2025. <https://www.semtech.com/>
20. Kang J.-M. LoRa Preamble Detection With Optimized Thresholds. *IEEE Internet Things J.* 2023; 7: 6525–6526. <https://ieeexplore.ieee.org/document/9997090>
21. Shaw J.A. Radiometry and the Friis transmission equation. *American Journal of Physics*. 2013; 81. <http://dx.doi.org/10.1119/1.4755780>
22. Announcement of the President of the Agency for Restructuring and Modernisation of Agriculture of 13 September 2024 (in Polish), 2024.
23. Ferreira, A.E., Ortiz, F.M., Costa, L.H.M.K. et al. A study of the LoRa signal propagation in forest, urban, and suburban environments. *Ann. Telecommun.* 2020; 75: 333–351. <https://doi.org/10.1007/s12243-020-00789-w>
24. Act of 12 July 2024, Electronic Communications Law (Journal of Laws 2024, item 1221) (in Polish), 2024. <https://isap.sejm.gov.pl/isap.nsf/DocDetails.xsp?id=WDU20240001221>
25. Public Information Bulletin of the Office of Electronic Communications (in Polish), 2024. <https://bip.uke.gov.pl/pozwolenia-radiowe/urzadenia-niewymagajace-pozwolenia/>
26. Attachment document for art. 1(3) to the decision of the European Commission: 2000/299/EC. <https://ec.europa.eu/docsroom/documents/40361>
27. Ai-Thinker. Ra-02 LoRa Product Specification. 2017.
28. Sinnott R.W. Virtues of the haversine, *Sky Telesc.*, 1984; 2: 159.
29. Geoinformatics services portal: Geoportal: www.geoportal.gov.pl